2000

State of the art large scale testing of ballast

Buddhima Indraratna
University of Wollongong, indra@uow.edu.au

D J Ionescu

Publication Details

Indraratna, B and Ionescu, D, State of the art large scale testing of ballast, In Railway Technical Society of Australasia (eds), CORE 2000 Railway Technology for the 21st Century, 2000, 24.1-24.13, Australia: Railway Technical Society of Australasia.

STATE-OF-THE-ART LARGE SCALE TESTING OF BALLAST

B. Indraratna[1], D. Ionescu[2] and H.D. Christie[3]

[1] Associate Professor, Dept. of Civil & Mining Engineering, University of Wollongong
[2] Doctoral Candidate, University of Wollongong and Lecturer, La Trobe University
[3] Principal Geotechnical Engineer, Geotechnical Services, Railway Services Australia

SUMMARY

Poor performance of rail roads is often associated with the loss of cross level, track profile and track alignment. The initial as placed condition of ballast and its engineering behaviour govern the stability and the performance of a railway track. The load bearing capacity of ballast and its short and long term degradation characteristics can only be studied using large scale testing equipment, because the conventional geotechnical equipment cannot accommodate the relatively large aggregates. Large-scale testing provides specific geotechnical knowledge on the shear strength and particle degradation of ballast, in relation to the particle size distribution. The influence of principal stress ratio on the deformation aspects of ballast is also investigated. The variation of shear strength, angle of internal friction, dilation rate and the degree of particle crushing at different confining pressures and principal stress ratios, are described by non-linear relationships that are different to conventional criteria developed for other granular materials. The University of Wollongong in collaboration with the Railway Services Australia (RSA) of NSW has initiated a major research project on railway ballast, where both static and dynamic testing of ballast are being conducted. The settlement characteristics of railway ballast were also studied in the laboratory, by simulating the correct axle loads of trains. The static behaviour was evaluated using a large scale triaxial apparatus and consolidometer, while the dynamic behaviour was investigated using a cubicle triaxial rig. The role of particle degradation, number of load cycles and the degree of wetting is discussed in relation to the settlement.

1 INTRODUCTION

Frequent congestion of main highways and the demand for quicker and safer transport have made the railways the most demanded means of public transportation in New South Wales (NSW). Ballast degradation and track deformation is clearly associated with increased train frequency and the passenger loads, leading to significantly high maintenance costs. In many countries including North America, a large proportion of the railways maintenance budgets is spent on ballast replacement and related activities (Chrismer, 1985). For example, in NSW, approximately 1.3 million tonnes of ballast was consumed at a cost of over 12 million dollars during the 1992-1993 period (Ionescu et al, 1996). Unless the proper role of geotechnical parameters which control the ballast stress-strain behaviour under static and repeated loads is carefully examined, the cost of maintenance cannot be reduced.

The conventional triaxial apparatus is one of the most versatile laboratory methods for obtaining the deformation and strength properties of fine-grained materials or small rock specimens. Nevertheless, the disparity between the actual particle sizes in the field and the greatly reduced particle sizes used in conventional laboratory equipment contributes to inaccurate deformation behaviour and failure modes, because of the inevitable size-dependent dilation and different mechanisms of particle crushing (Indraratna et al., 1998). To overcome these size-dependent problems, 'large-scale' triaxial facilities for testing ballast have been designed and built in-house at University of Wollongong. Naturally, these testing rigs provide more realistic information on the ballast stress-strain and degradation characteristics, using the prototype rock fragments. This paper elucidates the results from this major testing program conducted at the University of Wollongong in collaboration with the Railway Services Authority (RSA) of NSW, where static and dynamic testing of ballast (latite basalt) are being conducted.

The deformation and degradation of ballast under dynamic loading was studied using a large scale, cubicle triaxial equipment designed by the authors. In real railway tracks, lateral displacement of ballast is not prevented, hence the cubicle triaxial rig with unrestrained sides provides an ideal facility for physical modelling of ballast deformation under dynamic loading. The role of (a) the magnitude and the variation of the applied

load and (b) the number of load cycles on the deformation and degradation of ballast is the main concern of the current study. The breakage of ballast under static loading could be easily evaluated using a large scale, consolidometer with greater confinement (rigid boundaries). It was found, that the degradation of ballast is increased by dynamic loading. However, the rate of settlement is reduced with the increase in the number of load cycles. The breakage of particles enhances subsequent plastic deformation, which contributes to unacceptable settlements.

1.1 Role of ballast foundation

A typical ballast foundation is composed of graded layers of rock fragments structurally integrated with the sleepers (timber or concrete). The composite ballast foundation should provide the optimum resiliency, thereby transmitting the imposed wheel loading to an acceptable depth of the foundation while preventing excessive settlement and lateral flow. The granular nature of ballast should also ensure efficient drainage of the track, so that no internal pore water pressures are allowed to develop.

The most critical stage in the life of a ballast foundation is immediately after construction, when the ballast is in its loosest state. While the passage of trains would cause further compaction of the ballast layer, additional settlements would occur due to excessive particle breakage. In the track, the major and minor principal stresses are the effective axial stress (σ_1') and the effective lateral stress (σ_3'). While the former is generated by the axle train load, the latter is provided by the friction of sleepers and the restraint due to shoulders and crib ballast. The axial and lateral stresses are directly influenced by the initial degree of compaction of ballast, apart from the ballast-structure interaction mechanics. In any case, the confining pressure applied to the ballast foundation is always small compared to the axial stress. It has been reported by Raymond and Davies (1978), that when a maximum static wheel load of 150 kN could treble due to rail or wheel defects causing high stress concentrations at sleeper/ballast interfaces, the confining stress would hardly develop over 140 kN/m^2.

2 LARGE SCALE TRIAXIAL TESTING

For the design of railway track structures, the accurate geotechnical properties of ballast must be available for the railway engineer. Tests on scaled down aggregates cannot be relied upon for the prediction of deformation parameters. Therefore, large-scale testing is imperative, wherein samples must be prepared according to the field grading and tested under stresses representative of the field situation. The current standard tests for quality assessment represent aspects of durability for accepting or rejecting a potential ballast specimen, but they are not directly related to the actual performance of the track, either in terms of load bearing capacity or acceptable settlements (Raymond et al., 1976). Physical properties of latite basalt used in the present study are given in Table 1, in comparison with the Australian Standard recommendations. While one may conclude that latite basalt is a suitable angular ballast with sufficient strength, the deformations associated with the breakage of sharp edges and corners is to be expected upon the passage of frequent trains.

The latite basalt was quarried from Bombo, NSW. The particle size distribution curves (gradations A and B) are illustrated in Figure 1, together with the recommended State Rail Authority specifications (shaded area). Gradations A and B are parallel to the upper limit and the lower limit of RSA specifications, respectively. The range of particles vary between 10mm and 55 mm. The sample size ratio for large scale cylindrical triaxial testing was about 5.7, as defined by the diameter of the triaxial specimen (300 mm) divided by the maximum particle dimension. It has been argued that as the sample size ratio approaches 6, the size effects become negligible (Marachi et al., 1972; Indraratna, et al. 1993).

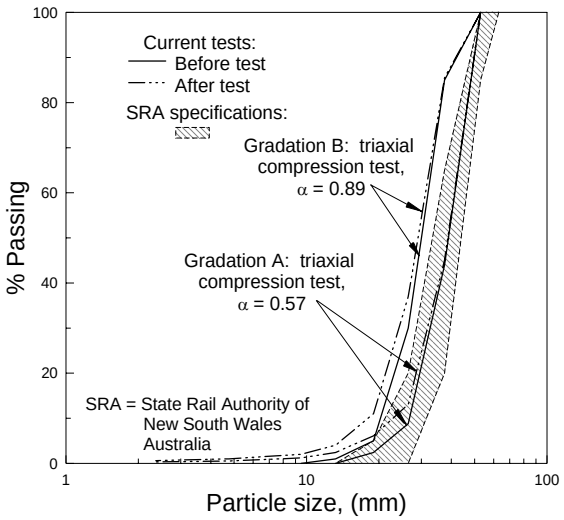

Figure 1 Particle size distribution of Latite Basalt (SRA, 1983; Indraratna et al, 1998)

Apart from the uniformity coefficient C_u (1.5-1.6 for both gradations), the modulus of gradation (α) has been utilised to describe the particle size distributions ($\alpha = 0.57$ for gradation A and $\alpha = 0.89$ for gradation B). This modulus of gradation (α) is a logarithmic function of the effective mean diameter of the consecutive pairs of sieves, and the weight of material retained on each pair of sieves (Hudson & Waller, 1969). The greater the content of fines, the higher the value of α.

Characteristic test	units	value	standard
Aggregate	%	12	< 25
L A Abrasion	%	15	< 25
Wet Attrition	%	8	< 6
Point load index	MPa	5.39	-
Crushing	MPa	130	-
Flakiness	%	25	< 30
Misshapen Particles	%	20	< 30

Table 1 Durability and Degradation Characteristics (Australian Standards, 1996)

Compaction of ballast was carried out to represent typical bulk unit weights in the field (15.3 - 15.6 kN/m^3), by imparting 25 blows from a standard Proctor hammer to each layer of ballast having a thickness of 50-60 mm. The relative densities for gradation A varied from 46 - 61%, and from 52 - 63% for gradation B. During laboratory compaction, a 4 mm thick rubber pad was used to minimise the risk of breakage of particles during impact.

A cylindrical triaxial apparatus (Fig. 2) which can accommodate specimens of 300 mm diameter x 600 mm high, was used for testing the latite ballast. The main components of the apparatus are: the triaxial chamber, the axial loading unit, the air pressure and the water control unit, the pore pressure measurement system, axial deformation measuring device and the volumetric change measurement device (Indraratna et al., 1998). The pore water pressure variation was measured using a porous disc (25 mm x 12 mm) attached to the bottom of specimen and connected to a pressure transducer and a digital recorder. Each test sample was subjected to isotropic consolidation under a known (constant) cell pressure before increasing the axial stress. The volume change was monitored during consolidation and shearing in relation to the corresponding axial strain and the deviator stress. The volume change of the specimen was determined by a coaxial piston located within a small cylindrical chamber (connected to the main cell), in which the smooth piston moves upwards or downwards depending on volume increase or decrease.

The specimen was prepared inside a rubber membrane subjected to a small vacuum head of 0.2 kPa, placed within a split cylindrical mould, which was removed before placing the sample within the cell pressure chamber. The sample deformation under this vacuum head was insignificant. The stress measurements were corrected to the membrane effect using the standard geotechnical practice (Bishop and Henkel, 1962).

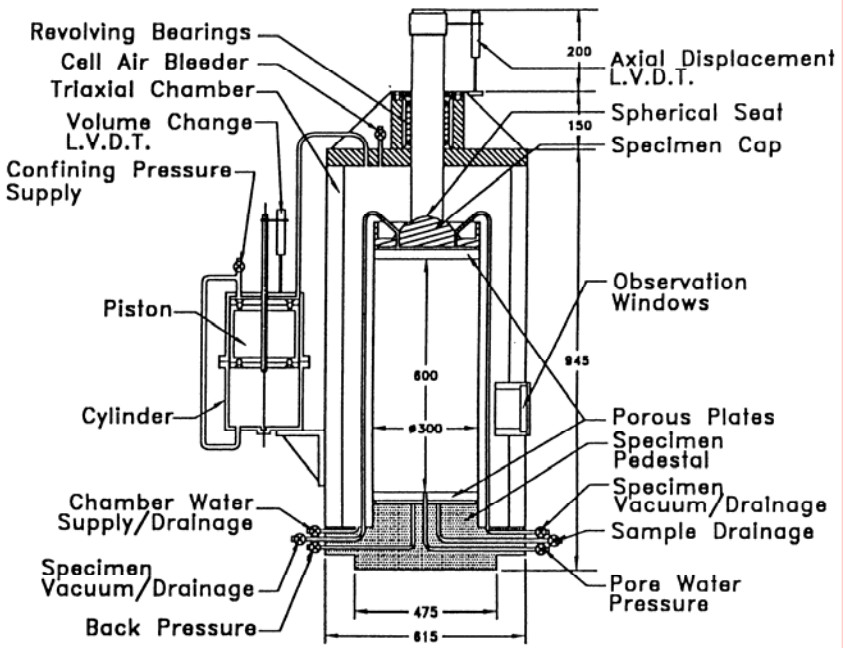

Figure 2 Large scale triaxial equipment

Prior to testing, each specimen was saturated by an upward flow of water from the bottom plate to represent 'wet' ballast, not uncommon in some of the low-lying coastal areas of NSW. Fully drained compression tests were conducted at relatively low confining pressures (10-240 kPa), simulating the typical lateral confinement within the ballast bed during the passage of unloaded to fully-loaded trains. In this study, all tests were carried out at an axial strain rate of 0.7% per minute allowing rapid pore pressure dissipation.

2.1 Triaxial Stress-strain Behaviour

Unlike in the case of sand or granulated fine media, no distinct failure plane was eminent even after 20% straining (post-peak), in the case of ballast specimens. For ballast, 'failure' can only be described by the behaviour at the peak deviator stress $(\sigma_1' - \sigma_3')_p$, and the mode of failure is considered to be 'bulging'. The typical results of isotropically consolidated drained triaxial tests (gradations A) are shown in Fig. 3. Gradation B (smaller particles than Gradation A, see Fig. 1) indicated a similar behaviour (data not shown here), although the principal stress ratios obtained for Gradation B were slightly larger than those of Gradation A, indicating the enhanced strength attributed to greater interlock of smaller particles. Similar to most granular media, (a) the principal stress ratio increases and (b) volumetric strain decreases (Fig. 3), with the increasing confining pressure (σ_3') at all axial strains. The post-peak behaviour is characterised by a strain-softening behaviour.

The variation of sample strains with confining pressure is plotted in Fig. 4, where dilation (volume increase) is seen to occur at low confining pressures. Obviously, the initial dilation is due to the radial expansion of the specimen (bulging) at low confining pressure ($\sigma_3' < 30$ kPa). However, the initially dilatant behaviour (at low σ_3') changes to an overall compaction for increased values of $\sigma_3' >$ 60 kPa. Moreover, the axial strain at peak deviator stress (i.e. failure strain) increases with the confining pressure (4% at σ_3' = 1 kPa to 14% at σ_3' = 240 kPa). The corresponding variation of the initial elastic deformation modulus ($E_i = \Delta(\sigma_1'-\sigma_3')/\Delta\varepsilon_a$) and the Poisson's ratio is shown in Fig. 5. Coarser particles (gradation A) indicate a greater axial strain upon initial loading (attributed to the larger porosity at compaction), thereby resulting in a smaller initial deformation modulus.

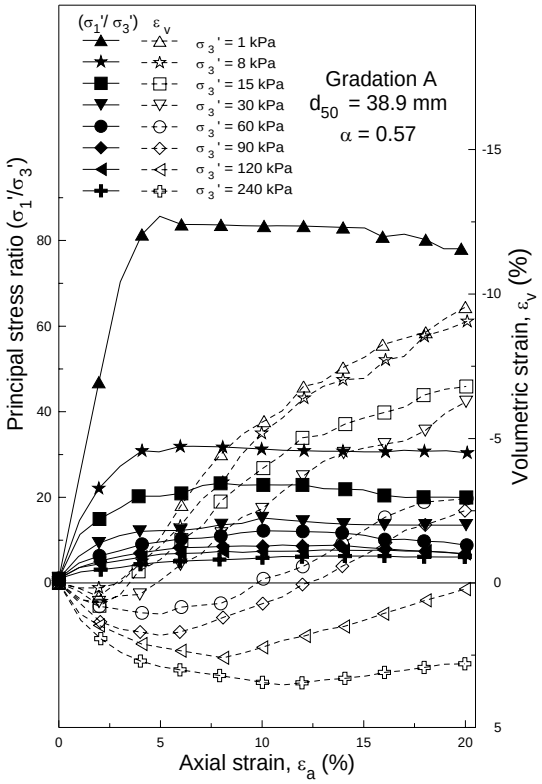

Figure 3 Drained compression tests at different confining pressure values on Latite Basalt (Indraratna et al, 1998)

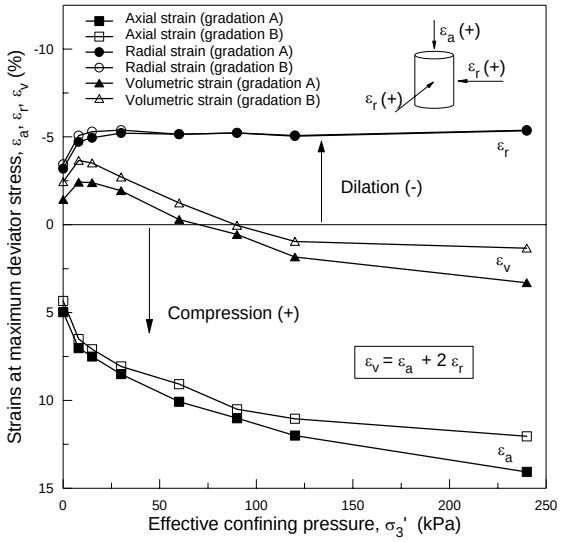

Figure 4 Variation of sample strains at peak deviator stress with confining pressure and grain size (Indraratna et al, 1998)

2.2 Shear Strength

Holtz and Gibbs (1956) have shown that irrespective of the size of triaxial test specimens, the quarried rock fragments (angular) exhibit considerably higher shear resistance in comparison with relatively

rounded river pebbles. Based on tests carried out on various rockfill materials, previous studies have shown that larger the particle sizes, greater the axial stress at failure at the same confining stress (Marsal, 1967, 1973; Marachi et al, 1972; Charles and Watts, 1980). The results railway ballast are plotted together with rockfill in Fig. 6, noting that the current tests on latite basalt were carried out at relatively low confining pressures. As expected, gradation B having a denser packing of particles shows a higher $(\sigma_1'/\sigma_3')_p$ in comparison with gradation A.

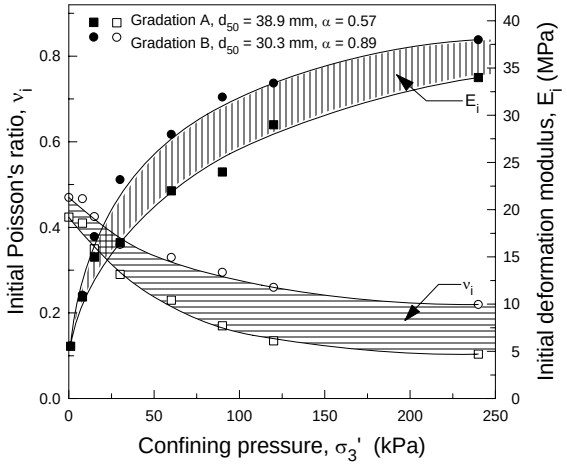

Figure 5 Influence of cell pressure on initial deformation modulus and Poisson's ratio in intial loading stage (Indraratna et al, 1998)

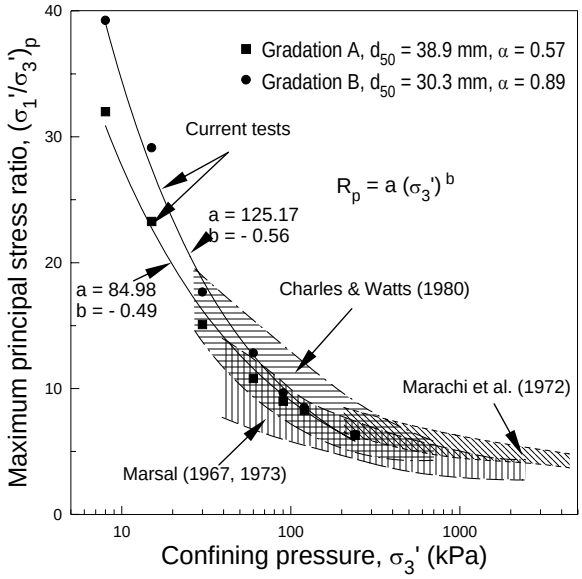

Figure 6 Influence of confining pressure on principal stress ratio at peak for Basalt in comparison with various granular media (Indraratna et al, 1998)

The shear strength of latite basalt can be represented by the Mohr-Coulomb circles, which indicate a non-linear strength envelope that is markedly curved and passing through the origin (results of Gradation A shown in Fig. 7). The non-linearity is pronounced at smaller confining pressures. The non-linear strength envelope is associated with the dilatant behaviour of rock fragments at low normal stress. Normal stresses below 400 kPa are usually representative of typical ballast foundations (Jeffs and Tew, 1991). The variation of apparent friction angle (ϕ_p') corresponding to the peak deviator stress is also plotted in Fig. 7. In railway ballast, where the confining pressure is low (hence, low normal stress), the apparent friction angle is expected to be relatively high ($\phi_p' > 40°$). The same material at relatively high confining pressure (i.e. rockfill in dams) will indicate a reduced friction angle in the order of 35°.

The shear strength of ballast is a function of the initial density (compaction) and the level of confining pressure generated on track. Indraratna et al (1993) proposed a dimensionless, non-linear strength criterion for rockfill, which can be extended to describe the behaviour of ballast at low confining pressure. This non-linear shear strength envelope is described by:

$$\tau_f/\sigma_c = m\,(\sigma_n/\sigma_c)^n \qquad (1)$$

where, σ_c is the uniaxial compressive strength of parent rock determined from the point load test, and m and n are dimensionless constants. The non-linearity of the strength envelope is governed by the coefficient n. The main advantage of Eqn. (1) is that by knowing the uniaxial compressive strength of the parent rock, the shear strength envelope can be estimated for a given railway ballast based on the empirical m and n coefficients. The test data for latite basalt in a normalised form are plotted in Fig. 8, in comparison with other sources of basalt used for railway construction. Irrespective of the compressive strength, particle sizes and gradations of different types of basalt, all test results fall within the defined lower and upper bounds. For small confining pressures (below 200 kPa), representative of rail tracks, n takes values in the order of 0.65 - 0.70.

2.3 Particle Degradation under Static Loading

In busy railway tracks, rapid fragmentation of the particles and the subsequent migration of fines 'clogging' the ballast voids are

commonly observed (Selig and Waters, 1994). The extent of particle crushing influences the deformation and the ultimate strength properties of ballast (Raymond et al., 1976; Jeffs and Marich, 1987). Particle breakage or degradation contributes to differential track settlement and lateral displacement. Although the actual crushing mechanisms are complex, it may be anticipated that initially, local crushing at interparticle contacts occurs, followed by the fracture of relatively weaker particles on further increase in load. The accumulation of fines and associated decrease in porosity of ballast with time can initiate undrained failures during and after heavy rainfall, at certain depths below the track surface.

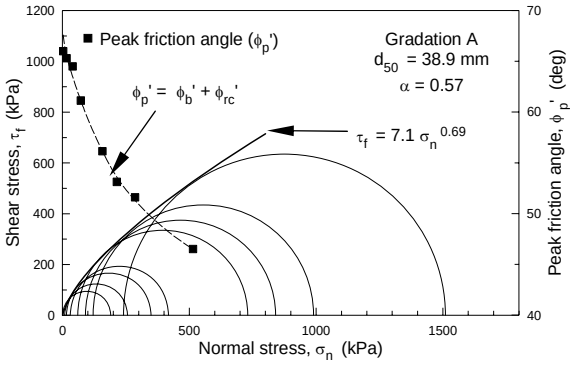

Figure 7 Mohr-Coulomb failure envelopes for Latite Basalt (Indraratna et al, 1998)

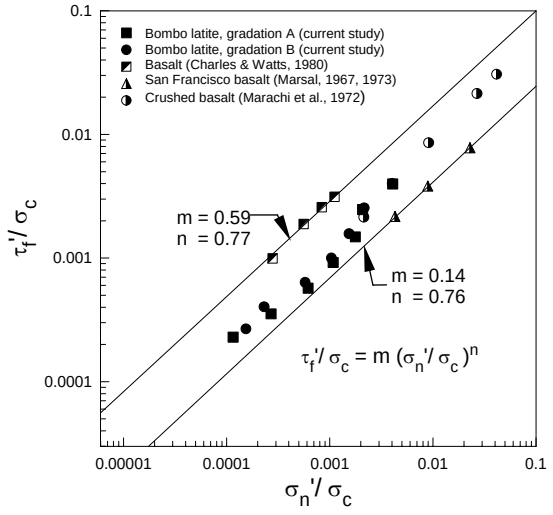

Figure 8 Normalized shear strength-normal stress relationship for various aggregates (Indraratna et al, 1998)

The degradation characteristics of latite basalt with depth, were determined by the authors by dividing the test specimens into two equal layers (300 mm high), separated by a thin geotextile interface. The geotextile could prevent the downward migration of pulverised particles. After each test, the sample was sieved and the changes in the particle size distribution of both layers were recorded. Because small changes in particle sizes cannot be clearly illustrated in the conventional gradation plots such as Fig.1, an alternative plot was created, where the difference between the percentage by weight of each grain size fraction before and after the test (ΔW_k) is plotted against the aperture of the lower sieve corresponding to that fraction (Fig. 9). The particle breakage index (B_g) is equal to the sum of the positive values of ΔW_k, expressed as a percentage (Marsal, 1973). The greater extent of particle breakage seems to occur within the upper part of the specimen. Assuming that the load distribution is expected to be uniformly transmitted, the non-uniform particle degradation may be due to the localised stress concentrations caused by the ballast angularity. It may also be possible that the geotextile dividing the specimen into two layers could have acted as a 'strain barrier', subjecting the upper layer to a greater extent of shearing stress. The breakage affects mainly the larger grains (27–53 mm), and this degradation is pronounced at increased confining pressures (Fig. 9). In other words, relatively small aggregates subjected to smaller confining stresses are the least affected by crushing.

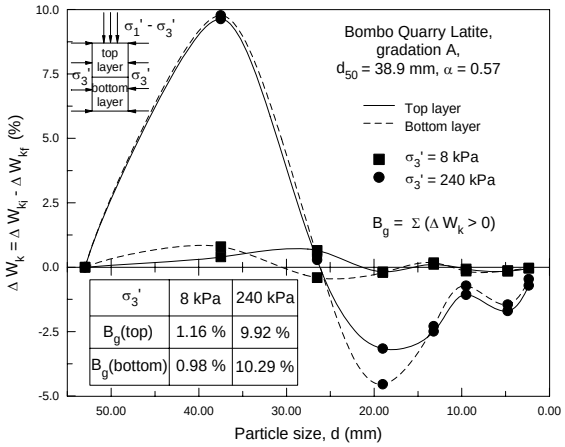

Figure 9 Variation of particle distribution with grain size for Bombo Basalt sheared at different confining pressures (Indraratna et al, 1998)

Figure 10 illustrates the relationship between the particle breakage index with the change in the maximum principal stress ratio and peak friction angle. As expected, a greater degree of breakage was observed for Gradation B (greater initial density). For latite basalt, knowing the applied principal stress ratio upon loading, the breakage index and the apparent friction angle can be conveniently estimated from Fig. 10. This information can then be

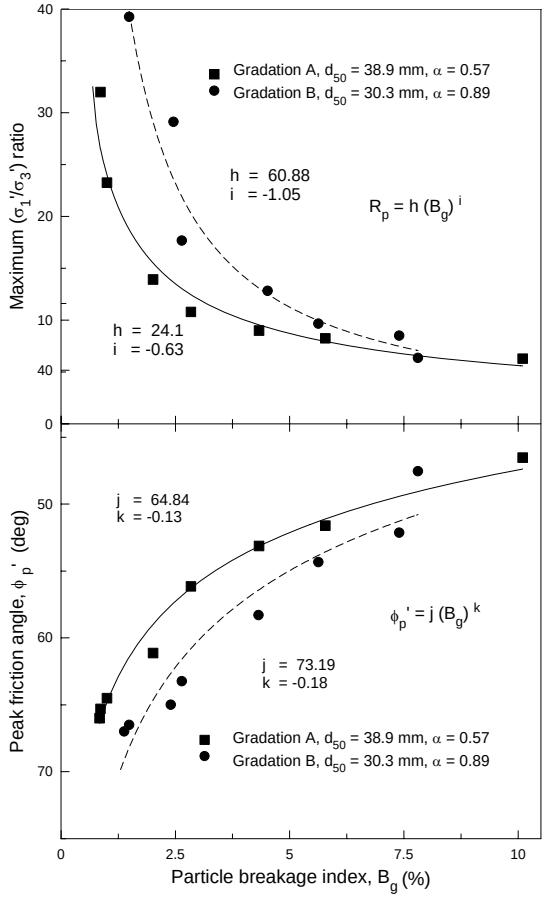

Figure 10 Effect of stress variation on particle breakage for Bombo Basalt (Indraratna et al, 1998)

translated to expected settlements and shear strength (bearing capacity) using other geotechnical means of analysis.

3 STATIC CONSOLIDATION OF BALLAST

Figure 11 illustrates the large scale, consolidometer used in this study. The ballast specimens were prepared to an average bulk unit weight of 13.8 kN/m^3 under loose slate, and up to about 15.6 kN/m^3 for the compacted ballast. The type of axial loading imposed on the sample was representative of the variable loading pattern in the field. In the Variable Load Increments (VLI) testing, a rapid initial load of 500 kPa, and subsequently, 50 kPa increments were applied at 2-hour intervals, followed by 100 kPa increments at hourly intervals. The maximum load of 950 kPa was maintained at a constant level for up to 24 hours, and then the ballast specimen was unloaded in 100 kPa decrements at 15 minute intervals. For the second type of compression tests (Constant Load Increments, CLI) a constant load increment of 100 kPa was applied at hourly intervals with a final increment of 150 kPa, until a maximum load of 950 kPa was attained. Subsequently, the sample was unloaded in the same manner as in the first set of tests.

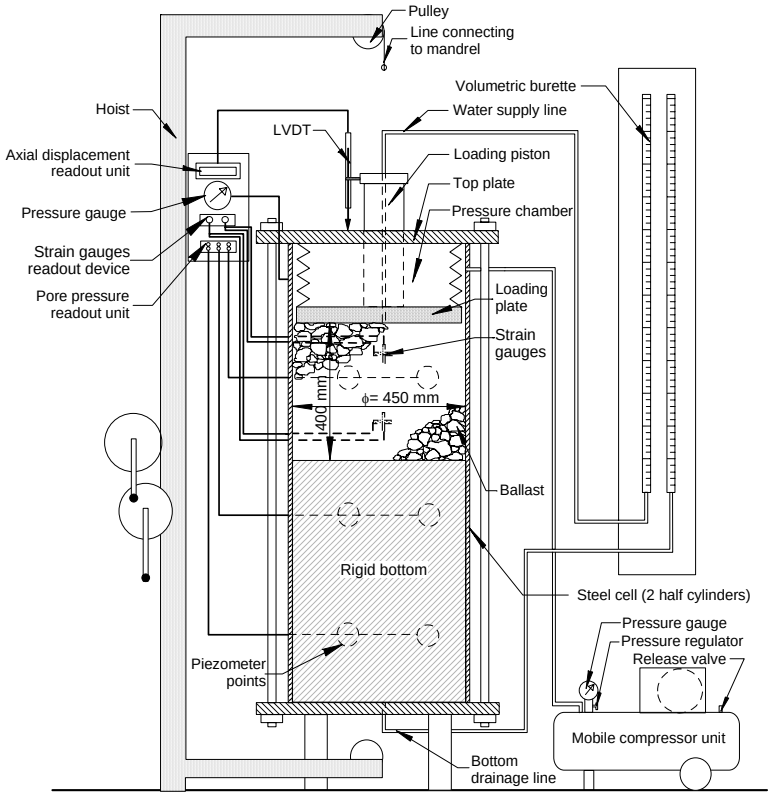

Figure 11 Large scale consolidometer for testing ballast

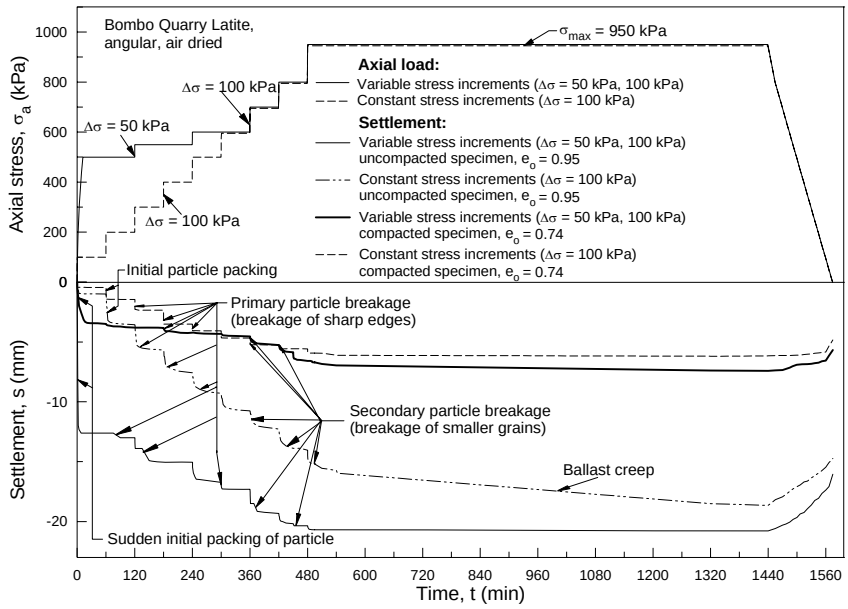

Figure 12 Settlement-time response for ballast, indicating particle breakage (Indraratna et al, 1997)

The associated settlements of uncompacted (e_o= 0.95) and compacted (e_o = 0.74) specimens for Variable Load Increments (VLI) and the Constant Load Increments (CLI) tests are illustrated in Fig.12. The rapid initial load of 500 kPa initiates a sudden settlement of 12.5 mm for the uncompacted specimen. The initial settlement of the compacted specimen was only about 3 mm. For the uncompacted ballast, significant creep takes place under the constant maximum loading (950 kPa), which is not significant for the compacted sample. As expected, while all samples indicate some rebound upon unloading, the rebound of the compacted samples was less pronounced. Irrespective of the type of loading and the associated particle degradation, the ultimate settlements tend to approach the same value for both initially compacted and uncompacted specimens.

3.1 Deformation under repeated loading

Repeated loading tests were also conducted for both uncompacted (e_o =0.95) and compacted (e_o =0.74) ballast specimens, for axial pressures varying from 50 to 560 kPa. The maximum pressure of 560 kPa in the laboratory was based on 30 tonne axle load and assuming a maximum train speed of 150 km/h. The calculations were based on the theory of 'beam on an elastic foundation' and assuming that one third of the sleeper length carries the wheel load (Jeffs and Tew, 1991). The minimum stress of 50 kPa models the effect of self-weight of rails, sleepers and crib ballast. The axial stress against the axial strain relationship for the compacted and uncompacted specimens under repeated loading is shown in Fig. 13. The axial strain significantly increases between load cycles for the uncompacted specimen. For the compacted specimen, most strain has already taken place after the first 2-3 cycles. Based on the corresponding settlement plots (Fig. 14), a theoretical prediction (Eqn 2) is also plotted for comparison.

$$s_N = s_1 (a \log N + 1) \qquad (2)$$

where, s_N = settlement at N number of cycles; s_1 = initial measured settlement after the first cycle; N = number of loading cycles; *a* = empirical coefficient determined by non-linear regression for available test data.

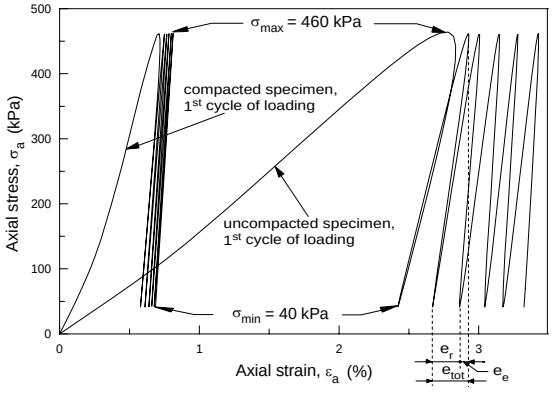

Figure 13 Stress-strain behaviour of loose and dense ballast under repeated loading unloading

For the ballast samples tested in this study, s_1 = 2.31 and 9.68 for compacted and uncompacted ballast, respectively. The empirical coefficient (*a*) for latite basalt is 0.345. For uncompacted ballast, Equation (3) underpredicts the settlements at initial load cycles, whereas the settlements are overestimated for N exceeding 100. The settlement predictions are acceptable for compacted ballast.

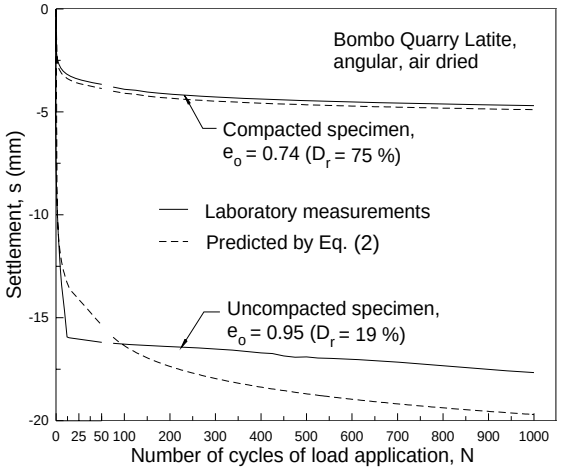

Figure 14 Effect of load cycles on settlement upon repeated loading

4 DYNAMIC LOADING AND BALLAST DEFORMATION

The deformation and degradation of ballast under dynamic triaxial loading was studied using a large scale, cubicle triaxial equipment. The cubicle apparatus with movable sides at University of Wollongong can accommodate large specimens of the size 800 x 600 x 600 mm (Fig. 15). The axial load is applied via a servo-hydraulic actuator through a 100 mm steel ram, and 2 pairs of hydraulic jacks with attached load cells provide the intermediate stress, σ_2 and the minor principal stress, σ_3 (i.e. lateral confining pressures). In the field, the lateral stresses (σ_2 and σ_3) model the restraint provided by the sleepers as the axle load is applied, and they are also related to the self-weight of shoulder and crib ballast. In the triaxial test, the minor principal stress (σ_3) is used to model the effect of self-weight of ballast (shoulders and adjacent crib), and the intermediate principal stress (σ_2) to model the transient stress between the sleepers and the self-weight of crib ballast. As no pore water pressures were considered (ballast is free draining), the total and effective stresses were assumed to be the same. The fully instrumented equipment enables the measurement of vertical and lateral pressures at various depths within the ballast bed, and the vertical and lateral displacements of the ballast specimens upon loading.

Upon vertical loading, the sides of the equipment are allowed to move with the lateral flow of ballast. Conventional cubicle testing chambers have rigid sides, which do not permit lateral displacement at the boundaries. In the field, lateral displacement of ballast is not prevented, hence, this facility (Fig. 15) is ideal for physical modelling of ballast deformation under realistic dynamic loading. The current test program was designed to determine the performance of latite basalt, in relation to the applied loading amplitude and the number of load cycles. In the past, total restraint due to the rigid cell walls has been a disadvantage in correctly simulating the particle degradation and associated settlements. Semi-confined devices (Jeffs and Marich, 1987; Norman and Selig, 1983) have simulated ballast deformation more accurately.

4.1 Specimen preparation and test procedure

The large triaxial box was filled in layers followed by the capping layer, and a rubber mat at the bottom of the box to provide sufficient subgrade reaction (resilience). The compaction of capping and ballast layers was carried out using a vibrating compactor simulating the field densities. Bulk unit weights of 16.7 KN/m^3 and 18.9 kN/m^3 were achieved for the ballast and capping layers, respectively. Each compacted layer was not more than 70 mm in thickness, and ballast breakage during compaction was prevented by placing a rubber mat on top of each layer.

The vertical load was applied to a timber sleeper segment in the triaxial box, representing the stresses generated in the field by 25 tonne and 30 tonne axle wheel loads, which translate to 73 kN and 88 kN, respectively, in the laboratory. The tests were conducted at a 15 Hz low-frequency level, maintaining a minimum seating load of 10 kN. The total number of cycles, up to one million, and the dynamic amplification were compatible with typical rail traffic of 60 MGT, and for train speeds of 80 kph. A number of reasons contribute to ballast settlement in the field. Selig and Waters (1994) indicated that the largest load has a dominant effect on track settlement. Shenton (1985) showed that the number of load cycles influences the settlements significantly, while Eisenmann et al, (1994) verified that high range frequencies associated with fast trains mainly increase

ballast settlements, based on field measurements.

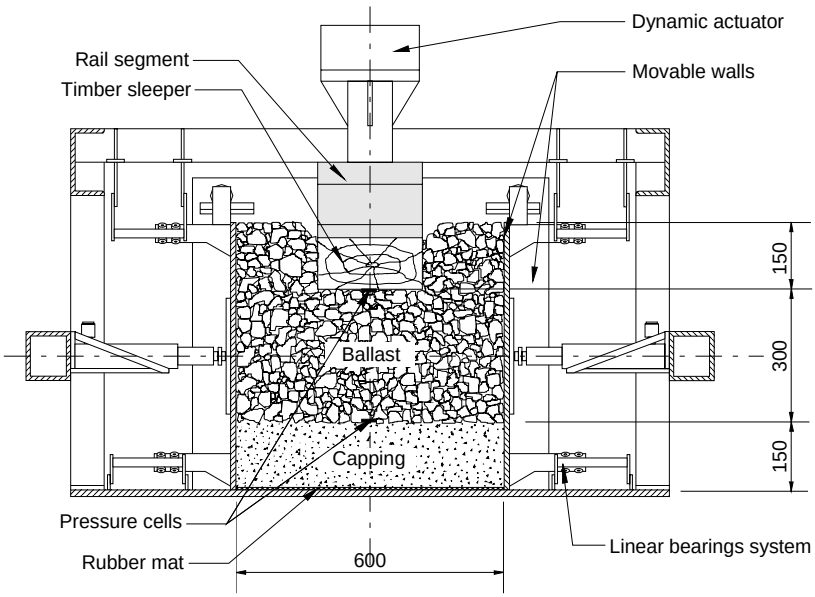

Figure 15 Cubicle triaxial testing rig with dynamic loading

4. 2 Ballast settlement

Behaviour of ballast under repeated loading (up to 1000 cycles) and dynamic loading (up to 10^6 cycles at 15Hz frequency) is non-linear. Under dynamic loading, the initial settlement is rapid during the first 10000-20000 cycles. This is purely due to the dynamic compaction of aggregates (stabilisation phase) which also takes place on new tracks or on recently repaired (maintained) track. The rapid initial settlement is followed by gradual consolidation with increasing number of load cycles, as shown in Fig. 16. During this consolidation phase, irregularities (e.g. sharp edges etc.) of larger particles break off causing an increased degree of packing, and then the particle-to-particle contacts are intensified. Upon further loading, additional settlements were accumulated at a diminishing rate when crushing and breakage of further angularities take place, which can be considered as secondary degradation of smaller particles. It is also noted from Fig.16 that as the load is increased from 25 to 30 tonnes axle load, a rapid settlement of ballast occurs, and the subsequent settlements converge towards the ultimate settlement of the 30 tonnes/axle curve. The settlement of ballast under dynamic load was best modelled as a power-function of the number of load cycles:

$$s_N = a\, N^{b} \qquad (3)$$

where, s_N = settlement after N number of load cycles; N = number of load cycles; *a* = settlement after one load cycle; and *b* = empirical coefficient (non-linear regression). In the above equation, it is important to note that the variation of test parameters such as the applied load and degree of compaction only affects the coefficient a, whereas b remains relatively unchanged.

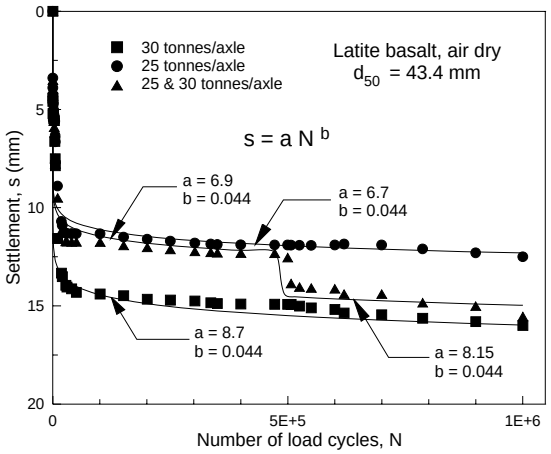

Figure 16 Effect of load cycles and axle loads on settlement

Field measurements indicate that the total settlement of railway tracks is a combined effect of the deformation of the various aggregate layers of the substructure (Selig and Waters, 1994). In order to evaluate the contribution of individual components (layers) of the laboratory model to the total settlement of the sleeper, the top level of the aggregate layers (i.e. ballast and capping) was measured at the end of every test. On the basis of laboratory measurements, it was

found that more than 60% of the total settlement was attributed to the deformation of ballast layer caused by cyclic loading, as indicated in Fig. 17.

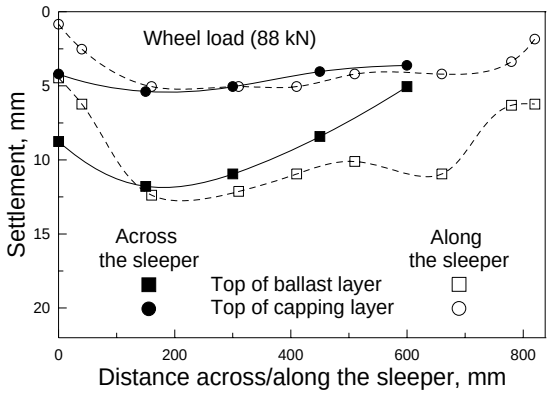

Figure 17 Settlement of ballast and capping layers in the cubicle rig

5 PARTICLE DEGRADATION IN DYNAMIC TESTING

In frequently used railway tracks in NSW, fragmentation and subsequent clogging of ballast voids with 'fouled' material is observed (Ionescu et al., 1996). It is anticipated that the particle size distribution curve will continue to change with the passage of trains due to particle degradation, hence the need for ballast maintenance becomes a costly exercise in overstressed railway tracks. In order to evaluate in the laboratory, the degradation characteristics of latite basalt, the crib ballast was separated from the top ballast using a geotextile. Such a fabric would prevent the migration of crushed particles towards the bottom of the ballast specimen during loading. After each test, the ballast specimen was removed from the testing equipment and carefully sieved to determine the difference of PSD curves above and below the geotextile interface.

It is evident from Fig. 18 that the breakage mainly affects the larger size particles in the order of 55 mm. The degree of crushing increases with the applied load. Irrespective of the load amplitude, the smaller particles suffer less degradation, and the degree of breakage is insignificant for the same range less than 10 mm. The grain breakage index (B_g) varies from 2.44% for tests run with 30 tonnes/axle to 1.51% for 25 tonnes/axle load.

6 EFFECT OF WETTING ON SETTLEMENT

As illustrated in Fig. 19, rapid settlement occurs upon wetting, and subsequently gradual creep takes place over a long period of time until the specimen is unloaded. The flooded specimen was loaded for up to 24 hours at an axial stress of 950 kPa. In comparison to the dry specimen (6.2 mm), the flooded specimen showed an increase in settlement of about 40%. This is partly due to the reduced interparticle friction leading to a more compact state, as well as due to material softening due to water, promoting further degradation. These results have direct implications on the field behaviour, where the loaded rail tracks can be subjected to increased settlement under saturated conditions. In low-lying coastal areas of NSW, certain tracks get partially submerged upon heavy precipitation.

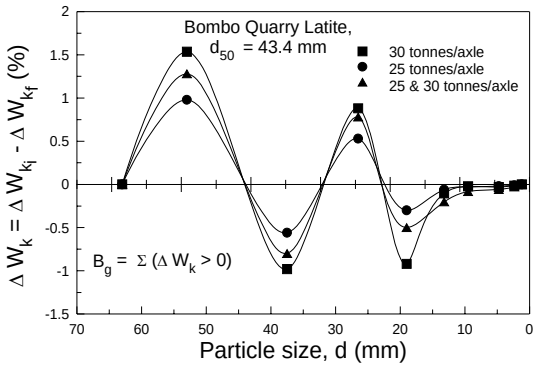

Figure 18 Grain breakage in dynamic triaxial testing

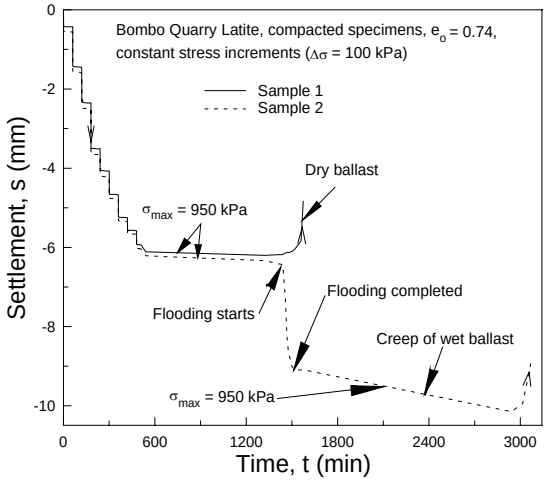

Figure 19 Effect of wetting on ballast settlement

7. CONCLUSIONS

The results of this study confirm that the amplitude and the nature of loading (constant, variable and repeated) determine the initial track settlement and the rate of settlement.

Irrespective of the nature of loading (static or dynamic), the ultimate settlement of the ballast converges to the same value. The initial settlement in particular is sensitive to the applied initial load. The static triaxial tests confirm that the shear and volume change behaviour of latite basalt at low confining pressure (< 100 kPa) varies significantly from the behaviour at larger confining pressure. The shear strength and the degree of particle degradation (crushing) are influenced by the particle size distribution, grain angularity, and the initial density.

The apparent friction angle of ballast is affected by the confining pressure, where pronounced non-linearity of the strength envelope is evident at small confining pressures. This suggests the importance of proper track design and maintenance by ensuring a full and compacted crib between the sleepers and shoulders at all times. The current study has introduced a modified shear strength criterion (non-linear) that incorporates the uniaxial compressive strength of the parent rock, which can be used for preliminary design of track. Laboratory data have shown that the enhanced dilatant behaviour of ballast at low levels of confining pressure is associated with an increase in the maximum principal stress ratio, and that the rate of dilatancy is further influenced by particle degradation. At elevated confining pressures (dilation is suppressed), the breakage index, B_g increases substantially.

Dynamic, cubical triaxial tests provide a more complete picture of load-settlement and particle degradation behaviour, because the speed and frequency of trains impart a quasi-cyclic load on the ballasted foundation, generating non-uniform vibrations. However, unlike in the case of homogeneous soils, specimens of rock aggregates require a larger number of tests to be conducted for obtaining realistic and reliable predictions. It is verified that particle sizes of 50-55mm undergo considerable degradation, while the smaller particles less than 15mm experience insignificant breakage.

Uniform optimum compaction of ballast decreases the differential settlements attributed to the train loads. The initial porosity of ballast directly affects the rate of settlements, for a given loading pattern. Moreover, the settlement increases substantially with the number of loading-unloading cycles as well as with the degree of saturation of ballast. For instance, it is concluded that up to 40% of the total settlements can be caused by flooding. Therefore, low-lying tracks which run the risk of flooding should be constructed to withstand greater settlements.

ACKNOWLEDGMENT

The authors wish to thank Mr Alan Grant and Ian Bridge (technical staff, University of Wollongong) for their assistance during the laboratory testing, and for the Railway Services Australia (NSW) for its support for this project.

REFERENCES

Australian Standards (1996). Aggregates and rock for engineering purposes. Railway ballast*, AS 2758.7 - 96*, Standards Australia, Sydney, NSW, Australia, 12 p.

Bishop, W. A. and Henkel D. J. (1962). *The measurement of soils properties in the triaxial test,* Edward Arnold (publishers) Ltd, London, 228p.

Charles, J. A. and Watts, K. S. (1980). The influence of confining pressure on the shear strength of compacted rockfill*, Geotechnique,* Vol. 30, No. 4, Inst of Civil Engineers, U. K., pp. 353-367.

Chrismer, S. M. (1985). Considerations of factors affecting ballast performance, *Report No.WP-110, Administration of American Railroads, Research and Test Department, Bulletin 704*, American Railway Engineering Association, pp. 118-150

Eisenmann, J., Leykauf, G. and Mattner, L. (1994). Recent developments in German Railway track design, ICE Trans. Transp., 105, 91-96.

Holtz, W. G. and Gibbs, H. J. (1956). Triaxial shear tests on pervious gravely soils*, J. Soil Mech. and Found. Engg.,* ASCE, Vol. 82, No. SM1, January, pp 1-22.

Hudson, S. B. and Waller, H. F. (1969). Evaluation of construction control procedures-aggregate gradation variations and effects, *National Co-Operative Highway Research Program, Report No. 69*, USA, p. 58.

Indraratna, B., Ionescu, D. and Christie, H. D. (1998). Shear behavior of railway ballast based on large scale triaxial tests, *ASCE Jnl. of Geotechnical and Geoenvironmental Engg.* Vol. 124, No. 5, May, pp. 439-449.

Indraratna, B., Ionescu, D., Christie, H.D. and Chowdhury, R.N. (1997). Compression and Degradation of railway Ballast under One-dimensional Loading. Australian

Geomechanics, Vol. 32, December Issue, pp. 48-61.

Indraratna, B., Wijewardena, L. S. S. and Balasubramaniam, A. S. (1993). Large-scale triaxial testing of greywacke rockfill*, Geotechnique*, Vol. 43, No. 1, Inst of Civil Engineers, U. K., pp. 37-51.

Ionescu, D., Indraratna, B. and Christie, D. (1996). Laboratory evaluation of the behaviour of railway ballast under static and repeated loads, *Proc. 7th Australia New Zealand Conf. on Geomech.*, The Inst. of Eng. Australia, Adelaide, pp. 86-91.

Jeffs, T. and Marich, S. (1987). Ballast characteristics in the laboratory, *Conf. Railway Engg.*, Perth, Inst. of Engineers, Australia, pp. 141-147.

Jeffs, T. and Tew, G.P. (1991). *A Review of Track Design Procedures - Sleepers and Ballast,* Vol. 2, Railways of Australia, Melbourne, 205p.

Marachi, N.D., Chan, C.K. and Seed, H.B. (1972). Evaluation of properties of rockfill materials, *, J. Soil Mech. and Found. Engg.,* A.S.C.E., Vol. 98, pp. 95-114*.*

Marsal, R. J. (1967). Large scale testing of rockfill materials*, J. Soil Mech. and Found. Engg.,* ASCE, Vol. 93, No. SM2, March, pp. 27-43.

Marsal, R.J. (1973). Mechanical properties of rockfill*, Embankment Dam Engineering*, *Casagrande Volume*, Wiley, New-York, pp. 109-200.

Norman, G. M. and Selig, E. T. (1983). Ballast performance evaluation with box tests, AREA Bul. 692, Vol. 84, 207-239.

Raymond, G. P. and Davies, J. R. (1978). Triaxial test on dolomite railroad ballast*, J Soil Mech. and Found. Engg.,* A.S.C.E., Vol. 104, GT6, pp. 737-751.

Raymond, G. P., Lake, R. W. and Boon, C. J. (1976). Stresses and deformations in railway track, *CIGGT, Report No. 76-11*, Canadian Inst. of Guided Ground Transport, Queen's University Press, Ontario, 171 p.

Selig, E.T. and Waters, J.M. (1994). *Track Geotechnology and Substructure Management*, Thomas Telford Services Ltd., London, 428p.

Shenton, M. J. (1985). Ballast deformation and track deterioration, Track Tech. Conf., 253-265, Thomas Telford Services Ltd., London.

State Railway Authority of NSW (1983). Specification for supply of aggregate for ballast, *T.S. 3402 - 83*, 3p.